

Research Article

Inertial Effects on Finite Length Pipe Seismic Response

**Virginia Corrado,¹ Berardino D'Acunto,²
Nicola Fontana,³ and Maurizio Giugni⁴**

¹ C.I.R.A.M., Federico II University, 80134 Naples, Italy

² Department of Mathematics and Applications, Federico II University, 80125 Naples, Italy

³ Department of Engineering, University of Sannio, 82100 Benevento, Italy

⁴ Department of Hydraulic, Geotechnical and Environmental Engineering, Federico II University, 80125 Naples, Italy

Correspondence should be addressed to Virginia Corrado, virginia.corrado@unina.it

Received 28 September 2011; Accepted 26 October 2011

Academic Editor: Alexander Pogromsky

Copyright © 2012 Virginia Corrado et al. This is an open access article distributed under the Creative Commons Attribution License, which permits unrestricted use, distribution, and reproduction in any medium, provided the original work is properly cited.

A seismic analysis for soil-pipe interaction which accounts for length and constraining conditions at the ends of a continuous pipe is developed. The Winkler model is used to schematize the soil-structure interaction. The approach is focused on axial strains, since bending strains in a buried pipe due to the wave propagation are typically a second-order effect. Unlike many works, the inertial terms are considered in solving equations. Accurate numerical simulations are carried out to show the influence of pipe length and constraint conditions on the pipe seismic strain. The obtained results are compared with results inferred from other models present in the literature. For free-end pipelines, inertial effects have significant influence only for short length. On the contrary, their influence is always important for pinned pipes. Numerical simulations show that a simple rigid model can be used for free-end pipes, whereas pinned pipes need more accurate models.

1. Introduction

During seismic events, buried pipeline damages are due to a combination of hazards: permanent ground deformations (landslides, liquefaction, and seismic settlements) and wave propagation effects. The latter are characterized by transient strain and curvature in the ground, due to the travelling wave effects. For the analysis of wave propagation, Newmark [1] proposed a simple procedure considering a single travelling wave with a constant wave form. The author assumed that a buried pipeline follows rigidly the motion of the soil. Consequently, the maximum axial pipe strain is the same as the maximum axial ground strain.

Further studies [2–8] indicated that dynamic amplification plays a minor role in the response of continuous buried pipelines. Therefore, axial strains and curvatures of a buried pipeline at the passage of a seismic wave can be determined according to the static response of the pipe [9]. In [10] O'Rourke and El Hmadi developed a procedure to estimate the maximum axial strain for long straight of buried continuous pipes subjected to seismic propagation along the longitudinal axis. They concluded that if slippage between the pipe and the surrounding soil does not occur, the pipe strain is similar to the ground strain, according to the Newmark approach. On the contrary, if slippage occurs, the Newmark method provides very conservative values of the pipe axial strain. Others authors [11–16] studied seismic response of buried pipes schematizing the pipe as a beam on dynamic elastic foundation and the soil modeled as a bed of springs according to the Winkler model (BDWF—Beam on Dynamic Winkler Foundation).

Nevertheless, the above-mentioned procedures consider infinite length pipelines and hence fail to account for their effective lengths and any construction works (constraint conditions). In [17] O'Rourke et al. developed analytical relations for finite length pipe subjected to various combinations of end conditions (i.e., free end, pinned, or spring end) using the concept of pipe development length. De Martino et al. [18–20] and Corrado et al. [21–24] developed a pipe soil interaction model considering finite length pipe. By assuming a linear elastic soil and neglecting slippage at the pipe-soil interface, the model analyzes the dynamic behavior of a finite length pipeline taking into account the boundary conditions at its ends and the inertia forces (FLBDWF—Finite Length Beam on Dynamic Winkler Foundation). The pipeline was assumed to be continuous; that is, any variations between the characteristics of the pipe and those of the joints were assumed negligible.

According to the FLBDWF approach, in this paper numerical simulations are carried out to assess the pipe dynamic response, showing that the maximum pipe strain strongly depends on the length and constraint conditions. Results obtained considering free- and pinned- end conditions are compared with values inferred from models assuming infinite length pipe and/or neglecting the inertial terms. For free-end pipes, the obtained results agree with the values inferred from the above-mentioned models only for long pipes, whereas for short lengths the maximum pipe strain significantly reduces. For pinned ends, neglecting pipe inertia and considering infinite length pipe underestimates the axial strain, particularly for short pipes.

In Section 2, the equation governing pipe axial motion is introduced and the distribution of seismic waves used in numerical simulations is described. Section 3 is devoted to the analysis of quasi-static condition for finite length pipes with free and pinned ends. Finite length pipe behavior under dynamic condition is proposed in Section 4.

2. Axial Motions

Consider a pipe of length L , and let U and U_g be the axial displacements of the pipe and the soil, respectively. By assuming the Winkler model for the elastic soil-structure interaction (the shear stress induced in the soil is proportional to the relative movement between the pipe and the soil) and neglecting slippage at the pipe-soil interface, the governing equation for the axial motions can be written as

$$m \frac{\partial^2 U}{\partial T^2} - EA \frac{\partial^2 U}{\partial X^2} + K(U - U_g) = 0, \quad (2.1)$$

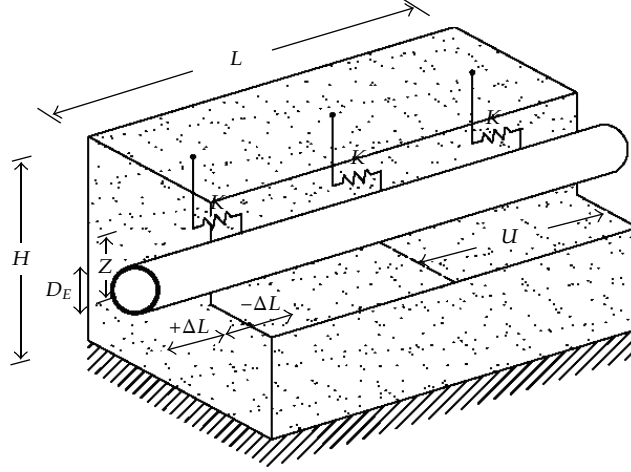


Figure 1: Soil-pipe interaction model.

in which X and T are space and time variable, m is the mass per unit length, E Young's modulus of the pipe material, $A = \pi s(D_E - s)$ the area of the pipe cross-section, where s and D_E are the thickness and the external diameter of the pipe, respectively, and $K = k_w \pi D_E$ the equivalent spring modulus, in which k_w is the soil's Winkler constant (Figure 1).

Because there are no accepted methods to predict the actual distribution of seismic waves [25], most authors assume the conservative hypothesis of Newmark, representing the soil motion by a single sinusoidal wave. The soil displacement parallel to the pipe can be written as

$$U_g = \begin{cases} U_{gm} \sin \omega \left(T - \frac{X}{V} \right), & \text{if } T > \frac{X}{V}, \\ 0, & \text{otherwise,} \end{cases} \quad (2.2)$$

where U_{gm} is the maximum soil displacement and ω is the angular velocity of oscillation of the seismic wave, given by $\omega = 2\pi f$, where f is the frequency and V is the apparent propagation velocity of the seismic wave. In [26, 27] O'Rourke et al. concluded that V is always greater than the propagation velocity V_S of the shear waves (S) in the soil's surface strata, equal to $V_S = (G/\rho)^{1/2}$, with G and ρ tangential elasticity modulus and soil density, respectively. They also proposed a method for determining the apparent propagation velocity, obtaining $V = 2.1$ km/s and 3.76 km/s for the 1971 San Fernando and 1979 Imperial Valley earthquake data, respectively. In [28] Committee on Gas and Liquid Fuel Lifelines considered that these values would be not appropriate for analysis, because they ignore changes in the wave shape from one point to other [15]. Consequently, in [14] Manolis et al. suggested for V values ranging between 1.2 and 3.0 V_S .

3. Neglecting Inertial Terms

3.1. Infinite Length Models

Several authors [2, 4, 8, 10] solved (2.1) neglecting the effects of inertia and assuming free field condition. According to these hypotheses, (2.1) becomes

$$\frac{\partial^2 U}{\partial X^2} - \frac{K}{EA}(U - U_g) = 0. \quad (3.1)$$

By assuming (2.2) for schematizing the soil motion and considering infinite length, the general solution is

$$U = BU_{gm} \sin \omega \left(T - \frac{X}{V} \right), \quad (3.2)$$

where

$$B = \frac{K/EA}{K/EA + (\omega/V)^2}. \quad (3.3)$$

In deriving (3.2), it has been tacitly assumed that U is bounded at infinity.

Pipe strain is equal to

$$\varepsilon = U_X = BU_{gX'}, \quad (3.4)$$

and the ratio between the maximum axial strain of the pipe and of the soil is

$$\frac{\varepsilon_{\max}}{\varepsilon_{g \max}} = B = \frac{K/EA}{K/EA + (\omega/V)^2}. \quad (3.5)$$

On this basis, the mentioned authors inferred the following conversion factor between pipe and soil strains

(i) Sakurai and Takahashi:

$$\frac{\varepsilon_{\max}}{\varepsilon_{g \max}} = \frac{1}{1 + (\omega/\omega_0)^2 (V_a/V)^2}; \quad (3.6)$$

(ii) Shinozuka and Koike:

$$\frac{\varepsilon_{\max}}{\varepsilon_{g \max}} = \frac{1}{1 + (2\pi/\lambda)^2 AE/K}; \quad (3.7)$$

(iii) Nagao et al.:

$$\frac{\varepsilon_{\max}}{\varepsilon_{g \max}} = \frac{1}{[2\pi/(\lambda_a \lambda)]^2 + 1}; \quad (3.8)$$

(iv) O'Rourke and El Hmadi:

$$\frac{\varepsilon_{\max}}{\varepsilon_{g \max}} = \frac{K/EA}{K/EA + [\pi/(2L_S)]^2}; \quad (3.9)$$

where $\omega_0 = \sqrt{K/\rho A}$, $V_a = \sqrt{E/\rho}$, λ is the effective wavelength of the seismic wave, $\lambda_a = \sqrt{K/EA}$, $L_S = \lambda/4$. Substituting all terms, we can notice that (3.6)–(3.9) yield the same conversion factor given by (3.3).

3.2. Finite Length Models

All the above authors consider infinite length pipeline and hence fail to account for the pipe length and end conditions. Neglecting inertial effects, in [17] O'Rourke et al. provided an upper-bound estimate for pipe strain (ε):

- (i) $\varepsilon = \varepsilon_g = V_{g \max}/V$, (the Newmark value), when the ground strain is small, the wavelength large, the soil relatively stiff and the pipe relatively flexible;
- (ii) $\varepsilon = t_u \lambda / 4EA$, when the ground strain is large, the wavelength small, the pipe is relatively stiff and the soil is relatively flexible,

where $V_{g \max}$ is the maximum horizontal ground velocity in the direction of wave propagation, t_u is the friction force per unit length at the soil pipe interface, equal to

$$t_u = \frac{\pi}{2} D_E \gamma H (1 + k_0) \tan(k\phi), \quad (3.10)$$

in which H is the cover atop the pipe, γ is the soil unit weight, ϕ the shear angle, k_0 and k the coefficient of lateral soil pressure at rest and the surface roughness factor [27]. The term L_d was introduced for assessing which equations to use. L_d represents the length over which soil friction forces must act to induce a given level of ground strain in the buried pipe, given by $L_d = EA\varepsilon_g/t_u$. It was assessed

$$\varepsilon = \begin{cases} \varepsilon_g = \frac{V_{g \max}}{V}, & \text{if } L_d < \frac{\lambda}{4}, \\ \frac{t_u \lambda}{4EA}, & \text{if } L_d > \frac{\lambda}{4}. \end{cases} \quad (3.11)$$

The equations are modified if the buried pipe has a buried facility at each end [17].

In this section we examine (3.1). The general solution takes the following form:

$$U = C_1U_1 + C_2U_2 + U_P, \quad (3.12)$$

where C_1 and C_2 are constants, U_1 and U_2 are the two independent solutions of the homogeneous equation, and U_P is the particular solution, that is, any solution to (3.1).

By assuming (2.2) for schematizing the soil motion and solving the corresponding homogeneous equation, the general solution of (3.1) is

$$U = C_1e^{X\sqrt{K/EA}} + C_2e^{-X\sqrt{K/EA}} + BU_{gm} \sin \omega \left(T - \frac{X}{V} \right), \quad (3.13)$$

with B arbitrary constant, provided by (3.3).

When considering finite length pipe (FLBDWF model), the constants C_1 and C_2 in (3.13) are nonzero and their respective values can be calculated according to the boundary condition. If the constraints at the pipe ends are such as to allow unrestrained deformation (free ends), the normal force is constant at $X = 0$ and $X = L$ and therefore

$$U_X = 0, \quad \text{for } X = 0, X = L, T > 0. \quad (3.14)$$

In this case, C_1 and C_2 can be calculated by solving the following system:

$$\begin{aligned} U_X(0, T) &= C_1\sqrt{\frac{K}{EA}} - C_2\sqrt{\frac{K}{EA}} - \frac{\omega}{V}BU_{gm} \cos \omega T = 0, \\ U_X(L, T) &= C_1\sqrt{\frac{K}{EA}}e^{L\sqrt{K/EA}} - C_2\sqrt{\frac{K}{EA}}e^{-L\sqrt{K/EA}} - \frac{\omega}{V}BU_{gm} \cos \omega \left(T - \frac{L}{V} \right) = 0. \end{aligned} \quad (3.15)$$

If the constraints at both ends of the pipe are such as to prevent all relative movement between the construction works and the pipe (pinned ends) we get

$$\begin{aligned} U &= U_{gm} \sin \omega T, \quad \text{for } X = 0, T > 0, \\ U &= \begin{cases} U_{gm} \sin \omega \left(T - \frac{L}{V} \right), & \text{if } T > \frac{L}{V}, \\ 0, & \text{otherwise,} \end{cases} \quad \text{for } X = L, T > 0. \end{aligned} \quad (3.16)$$

In this situation, C_1 and C_2 are given by the system:

$$\begin{aligned}
 U(0, T) &= C_1 + C_2 + BU_{gm} \sin \omega T = U_{gm} \cdot \sin \omega T, \\
 U(L, T) &= \begin{cases} C_1 e^{L\sqrt{K/EA}} + C_2 e^{-L\sqrt{K/EA}} + BU_{gm} \sin \omega \left(T - \frac{L}{V} \right) = U_{gm} \sin \omega \left(T - \frac{L}{V} \right), \\ \text{if } T > \frac{L}{V}, \\ C_1 e^{L\sqrt{K/EA}} + C_2 e^{-L\sqrt{K/EA}} = 0, & \text{otherwise.} \end{cases}
 \end{aligned} \tag{3.17}$$

The above systems are quasi-static: it is easy to determine the values of the two constants for the mentioned boundary conditions, as T varies. For free ends, C_1 and C_2 are given by

$$\begin{aligned}
 C_1 &= C_2 + \frac{\omega BU_{gm} \cos(\omega T)}{V\sqrt{K/EA}}, \\
 C_2 &= \frac{\omega BU_{gm} \left(\cos \omega(T - L/V) - e^{L\sqrt{K/EA}} \cos(\omega T) \right)}{V\sqrt{K/EA} \left(e^{L\sqrt{K/EA}} - e^{-L\sqrt{K/EA}} \right)},
 \end{aligned} \tag{3.18}$$

and, for pinned ends

$$\begin{cases} C_1 = -C_2 + (1 - B)U_{gm} \sin \omega T, \\ C_2 = \begin{cases} \frac{(1 - B)U_{gm} \left(e^{L\sqrt{K/EA}} \sin \omega T - \sin \omega(T - L/V) \right)}{e^{L\sqrt{K/EA}} - e^{-L\sqrt{K/EA}}}, & \text{if } T > \frac{L}{V}, \\ \frac{(1 - B)e^{L\sqrt{K/EA}} U_{gm} \sin \omega T}{e^{L\sqrt{K/EA}} - e^{-L\sqrt{K/EA}}}, & \text{otherwise.} \end{cases} \end{cases} \tag{3.19}$$

The pipe axial displacement and strain for the analyzed boundary conditions can be easily calculated by substituting the values of C_1 and C_2 in (3.13).

For analyzing the influence of length on pipe strain, consider a continuous buried steel pipe, whose characteristics are shown in Table 1. Since steel pipe is considered, welded joints allow to schematize as continuous the pipeline. It is assumed that the pipe strain results from seismic wave propagation due to shear waves (S waves) with peak ground velocity $V_{g \max} = 0.50$ m/s and an apparent propagation velocity with respect to the ground surface $V = 500$ m/s. Hence the maximum soil strain ε_g is equal to 0.001. All the above-mentioned procedures are applied to free-free and pin-pin end conditions. The calculations are carried out by assuming the backfill Winkler constant $k_w = 10.0$ N/cm³. The soil and wave characteristics are shown in Table 2.

In Table 3 the ratio R between the maximum axial strain of the pipe and of the soil is shown for three pipe lengths: 25 m, 150 m, and 250 m. The value of R depends on pipe length and boundary conditions: in particular, assuming finite length pipe with free ends and neglecting the inertial terms, the result obtained from the proposed approach for short pipe is

Table 1: Steel pipe characteristics.

$E = 2.1 \cdot 10^{11} \text{ N/m}^2$			
Diameter		Thickness	Weight per unit length
Nominal D_N [mm]	External D_E [mm]	s [mm]	[N/m]
600	609.6	9.5	1383

Table 2: Soil characteristics.

Backfill Winkler constant [k_w]	Shear wave velocity [V_S]	Apparent shear wave velocity [V]	Fundamental period of oscillation [T_g]	Angular velocity [ω]
10.0 N/cm ³	416.7 m/s	500 m/s	1.4 s	4.49 rad·s ⁻¹

Table 3: Ratio R between the maximum axial strain of the pipe and of the soil neglecting inertial terms.

L [m]	Infinite length	Finite length			
	Equations (3.6)–(3.9)	O'Rourke et al.		FLBDWF	
		free-free	pin-pin	free-free	pin-pin
25		0.0416	1.000	0.3001	0.9980
150	0.9846	0.2495	1.000	0.9846	0.9922
250		0.4158	1.000	0.9846	0.9922

lower than the value obtained with (3.6)–(3.9), which assumed infinite length pipe and tends to it for long pipe (250 m). On the contrary, the O'Rourke model yields values of R very low for the three lengths considered. For pinned ends, the FLBDWF model approximately tends to O'Rourke model, which coincides with the Newmark one in this case, for all pipe lengths.

4. Considering Inertial Terms

4.1. Infinite Length Models

In [15] Mavridis and Pitilakis solved (2.1) assuming the pipeline to be of infinite length and the soil homogeneous and viscoelastic. Under such assumptions, (2.1) can be written as

$$-EA \frac{\partial^2 U}{\partial X^2} + m \frac{\partial^2 U}{\partial T^2} + C \frac{\partial U}{\partial T} + KU = C \frac{\partial U_g}{\partial T} + KU_g, \quad (4.1)$$

where C is a damping factor. Without neglecting the inertial terms, the authors determined the following conversion factor between pipe and soil strain:

$$\frac{\varepsilon_{\max}}{\varepsilon_{g \max}} = \frac{K + i\omega C}{EA(\omega/V)^2 + K + i\omega C - m\omega^2}, \quad (4.2)$$

where $i = \sqrt{-1}$.

4.2. Finite Length Models

Unlike the models present in the literature, in [23] Corrado et al. consider the inertial terms in solving (2.1). By using the nondimensional variables x , t , and $u(x, t)$, defined by

$$x = \frac{X}{a} = \frac{X}{\sqrt{EA/K}}, \quad t = \frac{T}{b} = \frac{T}{\sqrt{m/K}}, \quad u = \frac{U}{U_{gm}}, \quad (4.3)$$

and the notations $u_{xx} = \partial^2 u / \partial x^2$, $u_{tt} = \partial^2 u / \partial t^2$, (2.1) is rewritten as

$$u_{tt} - u_{xx} + u = u_g, \quad (4.4)$$

in which the forcing term u_g is given by

$$u_g = \begin{cases} \sin \omega \left(bt - \frac{ax}{V} \right), & \text{if } bt > \frac{ax}{V}, \\ 0, & \text{otherwise.} \end{cases} \quad (4.5)$$

Equation (4.4) was integrated with reference to the two boundary conditions (3.14) and (3.16), which become

$$u_x = 0, \quad \text{for } x = 0, x = l, t > 0, \\ u = \sin \omega bt \quad \text{for } x = 0, t > 0, \quad u = \begin{cases} \sin \omega \left(bt - \frac{al}{V} \right), & \text{if } bt > \frac{al}{V}, \\ 0, & \text{otherwise,} \end{cases} \quad \text{for } x = l, t > 0, \quad (4.6)$$

where $l = L/a$ is the nondimensional pipe length.

The pipe is initially at rest, hence the problem is completed with the following initial conditions:

$$u = 0, \quad u_t = 0, \quad \text{for } 0 \leq x \leq l, t = 0. \quad (4.7)$$

By considering a model problem with known analytical solution, three methods were tested [23]: MacCormack (MC), Crank-Nicolson (CN), and Courant-Friederichs-Lewy (CFL) [29]. All methods show an excellent agreement of both U and U_x with the exact solution in the case of free ends pipe. On the contrary, for pinned ends the above-mentioned methods showed a different behavior in computing the axial strain. The methods provided results in good agreement with the exact solution U , whereas both MC and CN methods are unsatisfactory for the partial derivative. As an example, in Figures 2 and 3 strains at the time $T = 0.001$ s are given for a steel pipe of length $L = 25$ m, whose characteristics are shown in Table 1.

The calculations are carried out by considering the soil of Table 3 and ΔX equal to 0.01 m. Both free- and pinned-end conditions are simulated. Note that for free ends the

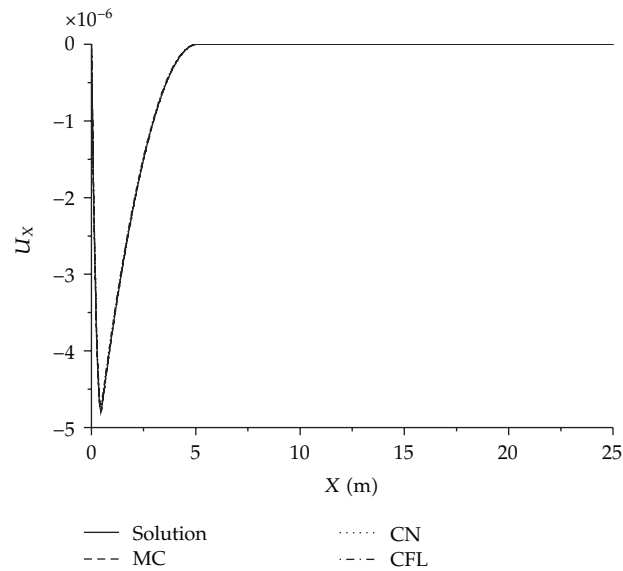


Figure 2: Approximated and exact solutions: U_X (free-end pipe).

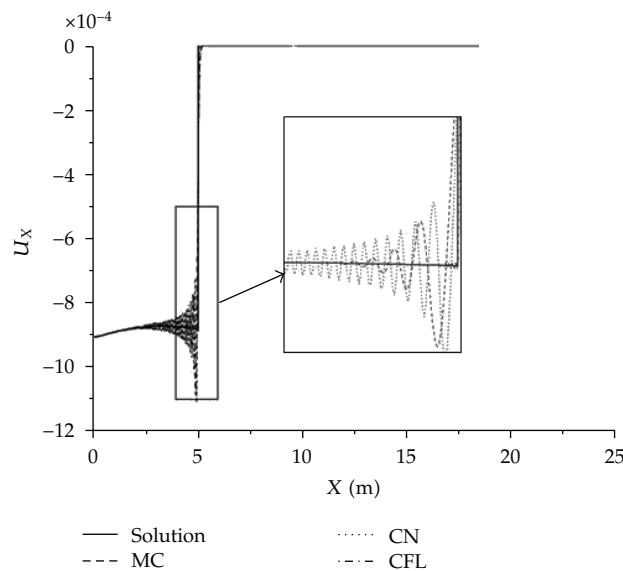


Figure 3: Approximated and exact solutions: U_X (pinned pipe).

results concerning U_X agree very well with the exact solution: all three methods show a good accuracy, since there are no discontinuity points. With reference to pinned ends, the axial strain $U_X = \varepsilon$ is discontinuous on the wave front; hence much attention is required. U_X is approximated with great accuracy by CFL method, whereas both MC and CN methods show undesirable oscillations for the strain close to the discontinuous points. Note that strain

Table 4: Ratio R between the maximum axial strain of the pipe and of the soil.

L [m]	No inertial terms				Inertial terms			
	Infinite length Equations (3.6)–(3.9)	Finite length		Infinite length		Finite length		
		O'Rourke et al. free-free	pin-pin	FLBDWF free-free	pin-pin	Mavridis and Pitolakis	FLBDWF free-free	pin-pin
25		0.0416	1.000	0.3001	0.9980		0.3021	1.2844
150	0.9846	0.2495	1.000	0.9846	0.9922	0.9847	0.9792	1.2053
250		0.4158	1.000	0.9846	0.9922		0.9861	1.1955

rather than displacement influences pipe seismic response. Seismic-induced stress can indeed be calculated according to the following relation:

$$\sigma = E\varepsilon, \quad (4.8)$$

and it can dramatically increase the pipe tensional state. Thus, the Courant-Friederichs-Lewy method is used to analyze the dynamic response of a continuous pipe.

A comparison between all the above-mentioned models is developed for the two boundary conditions applied to a continuous buried steel pipe, whose characteristics are shown in Table 1. In Table 4 the ratio R between the maximum axial strain of the pipe and of the soil is shown. When assuming infinite pipe length, R takes similar values in both situations: accounting for inertial terms as well as neglecting inertial terms. By considering finite pipe, R strongly depends on the pipe constraints and length. For free ends, the FLBDWF model applied considering inertial terms yields values that agree very well with those inferred from the FLBDWF applied neglecting pipe inertia, regardless of the length. On the contrary, pinned pipes present strains always greater than soil ones. R reduces at increasing pipe length. So, for free pipes the FLBDWF model yields same values both considering and neglecting the inertial terms. For pinned pipes the values are different, in particular, R is greater when the inertial terms are taken into account. This can be explained considering Figures 4 and 5, where pipe strains are plotted as X varies for four time values and for both boundary conditions. Note that for pinned-end pipe the strain is discontinuous on the wave front, as above mentioned. This discontinuity depends on pipe (m, D_E), soil (k_w), and earthquake (ω) characteristics. In Figure 6, R was plotted as pipe weight per unit length varies. Note that when pipe weight per unit length reduces, R tends to the value obtained applying the FLBDWF model neglecting the inertial terms, that is, to the value inferred from a rigid model. Then, when considering infinite pipe, the models available in the literature, both those that neglect and those that account for pipe inertia, underestimate seismic strain for pinned pipes, above all for short lengths.

The results confirm that the pipe behavior under seismic action is strongly influenced by the boundary conditions and pipe length. From a technical point of view, the rigid model allows a conservative estimation of the seismic strain for free-end pipe, since the maximum ground strain exceeds the maximum pipe strain. That is not true for pinned pipes, for which only a FLBDWF can properly account for the actual boundary condition. An infinite length model could underestimate the maximum strain when the pipes are ground-anchored, thus leading to unsafe design.

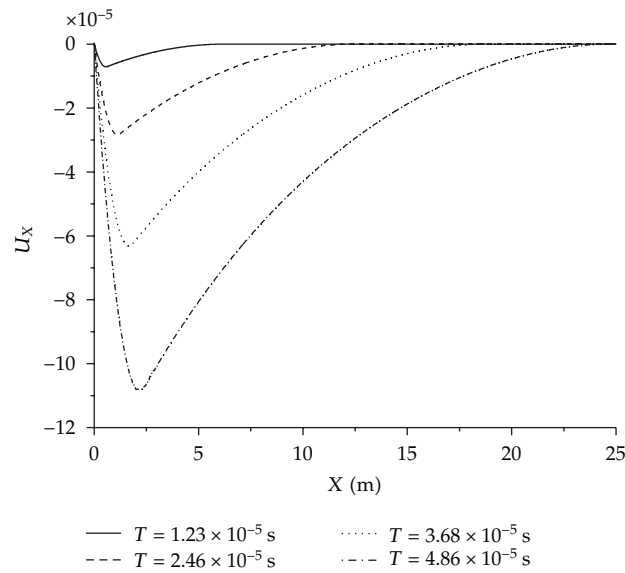


Figure 4: Pipe strain as X varies (free-end pipe).

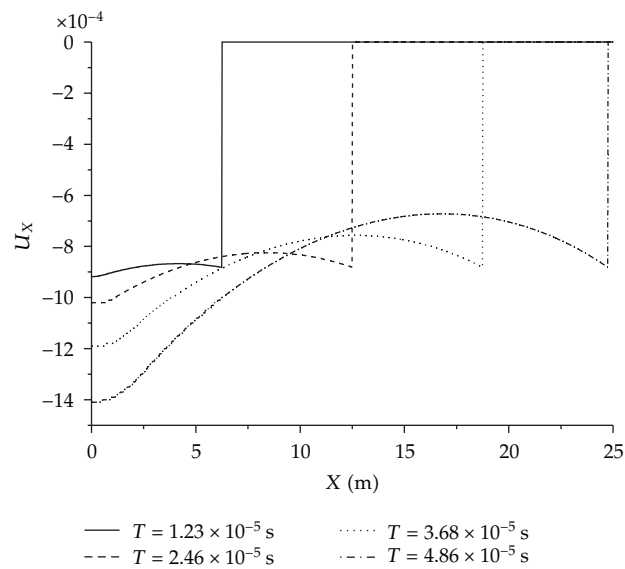


Figure 5: Pipe strain as X varies (pinned pipe).

5. Conclusions

In the present paper, the authors analyze the effects of seismic events on the axial motions of finite length continuous pipes taking into account inertial terms. Results show that the maximum strain of the pipe strongly depends on the pipe length and constraints. For free long pipes, the maximum pipe strain is slightly lower than the maximum ground strain. Within this range, the calculated strains are the same as the values inferred from the models

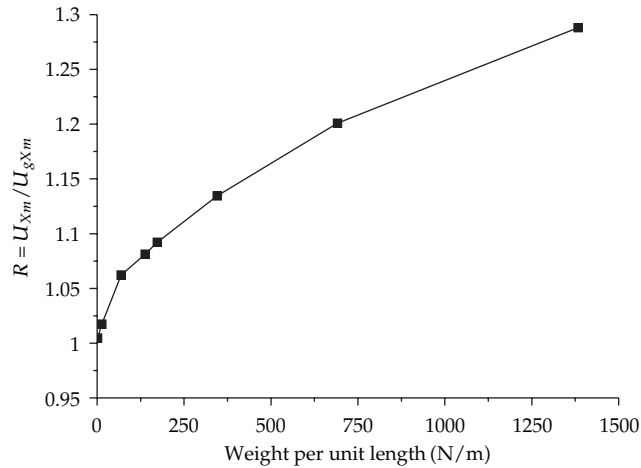


Figure 6: Ratio R between the maximum axial strain of the pipe and of the soil as weight per unit length varies (pinned pipe).

discussed by authors which assume infinite pipe and neglect the effect of inertia. On the contrary, the maximum pipe strain significantly reduces as the pipe length reduces. Therefore numerical results emphasize that for free-end pipes a BDWF (or rigid) model can be applied for long pipes.

For pinned pipes, the rigid model underestimates the axial strain. According to the proposed approach, the maximum pipe strain strongly exceeds the soil strain and hence the FLBDWF model allows a more accurate estimate of the pipe seismic stress considering pipe length, boundary conditions, and inertial terms.

References

- [1] N. M. Newmark, "Problems in wave propagation in soil and rocks," in *Proceedings of the International Symposium on Wave Propagation and Dynamic Properties of Earth Materials*, pp. 7–26, University of New Mexico Press.
- [2] M. Sakurai and T. Takahashi, "Dynamic stresses of underground pipelines during earthquakes," in *Proceedings of the 4th World Conference on Earthquake Engineering*, pp. 81–95, Santiago, Chile, 1969.
- [3] R. A. Parmelee and C. A. Ludtke, "Seismic soil-structure interaction of buried pipelines," in *Proceedings of the U. S. National Conference on Earthquake Engineering*, EERI, Ann Arbor, Mich, USA, 1975.
- [4] M. Shinozuka and T. Koike, "Estimation of structural strains in underground lifeline pipes. Lifeline earthquake engineering—buried pipelines, seismic risk, and instrumentation," *ASME*, vol. 34, pp. 31–48, 1979.
- [5] R. Parnes and P. Weidlinger, "Dynamic response of an embedded pipe subjected to periodically spaced longitudinal forces," Grant Report 13, National Science Foundation by Weidlinger Associates, 1979.
- [6] J. P. Wright and S. Takada, "Earthquake response characteristics of jointed and continuous buried lifelines," Grant Report 15, National Science Foundation by Weidlinger Associates, 1980.
- [7] I. Nelson and L. Baron, "Earthquakes and underground pipelines—an overview," Grant Report 17, National Science Foundation by Weidlinger Associates, 1981.
- [8] S. Nagao, S. Hoojyo, and T. Iwamoto, "Measures to protect buried pipelines from earthquakes and soft ground," in *Europipe 1982 Conference*, pp. 33–40, Basel, Switzerland, 1982.
- [9] American Society of Civil Engineers, "Guidelines for the seismic design of oil and gas pipeline systems," in *Technical Council on Lifeline Earthquake Engineering, Committee on Gas and Liquid Fuel Lifelines*, p. 473, ASCE, Reston, Va, USA, 1984.

- [10] M. J. O'Rourke and K. El Hmadi, "Analysis of continuous buried pipelines for seismic wave effects," *Earthquake Engineering & Structural Dynamics*, vol. 16, no. 6, pp. 917–929, 1988.
- [11] G. De Martino, G. de Marinis, and M. Giugni, "Risposta dinamica di tubazioni di drenaggio in zona sismica," *Idrotecnica*, vol. 1, pp. 13–25, 1994 (Italian).
- [12] G. De Martino and M. Giugni, "Seismic effects on waterworks," *Excerpta*, vol. 11, pp. 143–195, 1997.
- [13] G. De Martino, N. Fontana, M. Giugni, and G. Perillo, *I Grandi Collettori di Drenaggio in Zona Sismica*, Atti del IX Convegno Nazionale ANIDIS, 1999.
- [14] G. Manolis, K. Pitilakis, P. Telepoulidis, and G. Mavridis, "A hierarchy of numerical models for SSI analysis of buried pipelines," *Transactions on The Built Environment*, vol. 14, 1995.
- [15] G. Mavridis and K. Pitilakis, "Axial and transverse seismic analysis of buried pipelines," in *Proceedings of the 11th World Conference on Earthquake Engineering*, Acapulco, Mexico, 1996.
- [16] R. Viparelli, S. Santorelli, C. Cocca, and A. G. Pizza, *Dynamic Response of Large-Diameter Pipes Laid in Seismic Areas*, vol. 19, BEM, Roma, Italy, 1997.
- [17] M. J. O'Rourke, M. D. Symans, and J. P. Masek, "Wave propagation effects on buried pipe at treatment plants," *Earthquake Spectra*, vol. 24, no. 3, pp. 725–749, 2008.
- [18] G. De Martino, N. Fontana, M. Giugni, R. Greco, and G. Perillo, *Dynamic Behaviour of Continuous Buried Pipes Subject to Earthquakes*, SUSI, Wessex Institute of Technology, 2000.
- [19] G. De Martino, F. De Paola, N. Fontana, and M. Giugni, "Azioni dinamiche su tubazioni continue interrata in zona sismica," in *Atti del Congresso Nazionale "Condotte per acqua e gas"*, *L'Acqua*, vol. 1&2, pp. 134–140, 2002.
- [20] G. De Martino, B. D'Acunto, N. Fontana, and M. Giugni, "Dynamic response of continuous buried pipes in seismic areas," in *ASCE Pipelines Conference*, August 2006.
- [21] V. Corrado, B. D'Acunto, N. Fontana, and M. Giugni, "Risposta dinamica di tubazioni interrata in zona sismica," in *31st Convegno Nazionale di Idraulica e Costruzioni Idrauliche*, 2008.
- [22] V. Corrado, B. D'Acunto, N. Fontana, and M. Giugni, "Dynamic response of water networks in seismic areas," in *IABSE 17th Congress Chicago*, 2008.
- [23] V. Corrado, B. D'Acunto, N. Fontana, and M. Giugni, "Estimation of dynamic strains in finite end-constrained pipes in seismic areas," *Mathematical and Computer Modelling*, vol. 49, no. 3-4, pp. 789–797, 2009.
- [24] V. Corrado, B. D'Acunto, N. Fontana, and M. Giugni, "Effetti dinamici su condotte interrata in zona sismica," in *32nd Convegno Nazionale di Idraulica e Costruzioni Idrauliche*, 2010.
- [25] European Prestandard, ENV 1998–4, Design of structures for earthquake resistance Part 4: silos, tanks and pipelines, CEN, 81 pp, 2006.
- [26] M. J. O'Rourke, M. C. Bloom, and R. Dobry, "Apparent propagation velocity of body waves," *Earthquake Engineering & Structural Dynamics*, vol. 10, no. 2, pp. 283–294, 1982.
- [27] M. J. O'Rourke and X. Liu, "Response of buried pipelines subject to earthquake effects," MCEER Monograph 3, Multidisciplinary Center for Earthquake Engineering Research, University at Buffalo, Buffalo, NY, USA, 1999.
- [28] American Society of Civil Engineers, *Seismic Response of Buried Pipes and Structural Components*, Committee on Seismic Analysis, New York, NY, USA, 1983.
- [29] B. D'Acunto, *Computational Methods for PDE in Mechanics*, World Scientific, Singapore, 2004.



Hindawi

Submit your manuscripts at
<http://www.hindawi.com>

